

Low-Entropy States of Neutral Atoms in Polarization-Synthesized Optical Lattices

Carsten Robens, Jonathan Zopes, Wolfgang Alt, Stefan Brakhane, Dieter Meschede, and Andrea Alberti*

Institut für Angewandte Physik, Universität Bonn, Wegelerstrasse 8, D-53115 Bonn, Germany

(Received 8 August 2016; revised manuscript received 28 November 2016; published 8 February 2017)

We create low-entropy states of neutral atoms by utilizing a conceptually new optical-lattice technique that relies on a high-precision, high-bandwidth synthesis of light polarization. Polarization-synthesized optical lattices provide two fully controllable optical lattice potentials, each of them confining only atoms in either one of the two long-lived hyperfine states. By employing one lattice as the storage register and the other one as the shift register, we provide a proof of concept using four atoms that selected regions of the periodic potential can be filled with one particle per site. We expect that our results can be scaled up to thousands of atoms by employing an atom-sorting algorithm with logarithmic complexity, which is enabled by polarization-synthesized optical lattices. Vibrational entropy is subsequently removed by sideband cooling methods. Our results pave the way for a bottom-up approach to creating ultralow-entropy states of a many-body system.

DOI: [10.1103/PhysRevLett.118.065302](https://doi.org/10.1103/PhysRevLett.118.065302)

Introduction.—Compared to other quantum systems, ultracold atoms in optical lattice potentials stand out for being naturally scalable to a large number of particles. They offer thousands of sites, arranged in periodic arrays, in which quantum particles such as atoms can be confined and manipulated [1]. The idea of employing the myriad of sites available as a well-controlled Hilbert space has influenced modern research frontiers ranging from quantum metrology [2], quantum information processing [3–8], discrete-time quantum walks [9], up to quantum simulations of strongly correlated condensed-matter systems [10–12] with single lattice-site resolution [13,14]. Substantial experimental effort has recently been devoted to creating low-entropy states of atoms in the lattice, with each site being occupied by an integer number of atoms. Low-entropy states play an essential role in a host of quantum applications including the creation of highly entangled cluster states for quantum information processing [15], investigation of Hong-Ou-Mandel-like quantum correlations in many-body systems [16,17], and the quantum simulation of quantum spin liquids in frustrated systems [18,19].

To date, the standard approach to generate low-entropy states in optical lattices relies on a Mott insulator phase [10,11]. This is denoted as a top-down approach since ultracold atoms, due to interactions, self-organize in domains with integer filling factors. Other approaches [20] relying only on laser cooling techniques have recently demonstrated filling factors beyond the one-half limit imposed by inelastic light-assisted collisions [21,22], though without providing a fully deterministic method. In contrast, a bottom-up

approach generating arbitrary low-entropy states from individual atoms has long been desired [3,4], yet never been experimentally realized. In this Letter, we demonstrate a bottom-up approach to generate arbitrary atom patterns, including unity filling of lattice sites, in a one-dimensional (1D) optical lattice. Inspired by the seminal work by Jaksch *et al.* [3] proposing spin-dependent optical lattices to control individual atoms' positions, our work realizes the atom-sorting scheme proposed by Weiss *et al.* [23]. The experimental challenge consists in developing spin-dependent optical lattices able to shift atoms by any amount of lattice sites conditioned to their spin state. Previous implementations [24,25] of spin-dependent optical lattices were limited to only relative displacements of the two spin components and to relative shift distances of one site at most. To overcome these limitations, we have devised a scheme for spin-dependent transport based on a high precision, large bandwidth synthesizer of polarization states of light. Hence, we refer to our new implementation of spin-dependent optical potentials as polarization-synthesized (PS) optical lattices. PS optical lattices allow us to reposition individual atoms with a precision of 1 Å, reducing thereby the positional entropy of a randomly distributed ensemble to virtually zero. This is in stark contrast to the atom-sorting technique formerly demonstrated by our group [26], whose positioning precision was limited to about five sites. In addition, the novel approach requires no postselection, which has limited the success rates in earlier efforts to create ordered patterns from a thermal ensemble [27,28]. Very recently, similar results [29,30] have been obtained using atoms in movable arrays of optical tweezers, which appear particularly suited to exploit Rydberg interactions [31], as it suffices for them to sit at well localized positions spaced by relatively large distances [32,33]; in comparison, PS optical lattices, besides allowing matter waves to delocalize in space in highly stable optical potentials [34], also permit parallel sorting of atoms through the control of two spin species. Relying on that, we identify a sorting

Published by the American Physical Society under the terms of the [Creative Commons Attribution 4.0 International license](https://creativecommons.org/licenses/by/4.0/). Further distribution of this work must maintain attribution to the author(s) and the published article's title, journal citation, and DOI.

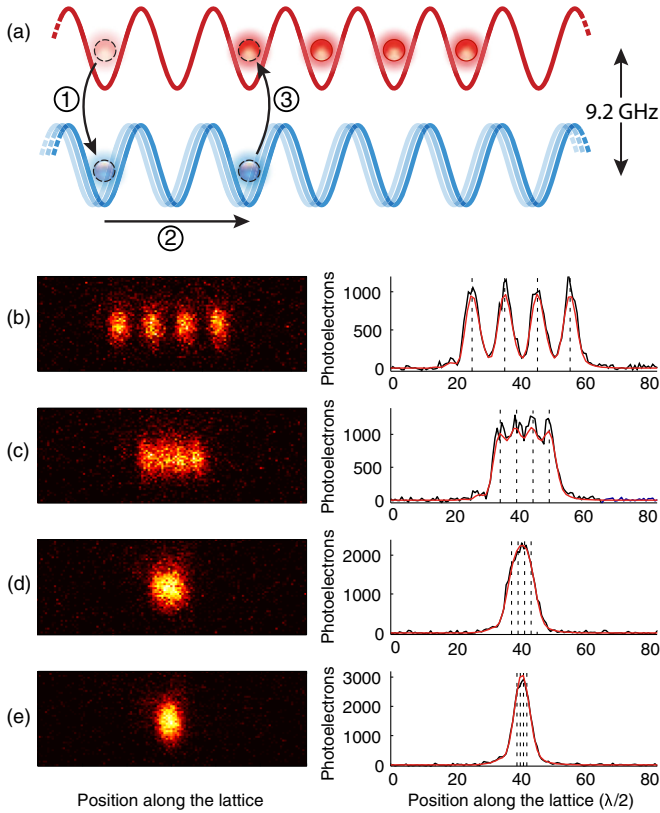


FIG. 1. Atom sorting in polarization-synthesized optical lattices. (a) Central building block of the atom-sorting procedure: (1) the leftmost atom (marked by dashed circle) is transferred from the *storage register* (upper lattice) into the *shift register* (lower lattice) by a microwave pulse, (2) transported by two sites to the right by shifting the lower lattice, (3) and transferred back into the storage register. (b)–(e) From top to bottom, four atoms deterministically placed at equidistant separations of $d_{\text{target}} = (10, 5, 2, 1)$ lattice sites. Left panels: Recorded single-shot fluorescence images. Right panels: Vertically integrated distributions (black lines) with the fitted intensity profiles (red curves) and the reconstructed positions (vertical dashed lines).

algorithm with logarithmic complexity, which allows in two dimensions a dramatic speed-up promising unity filling with thousands of atoms. Moreover, PS optical lattices directly allow one to investigate the dynamics of spinor quantum particles [35–37].

Atom sorting.—The principal result of this work is shown in Fig. 1: four ^{133}Cs atoms from a dilute thermal ensemble are rearranged into a predefined, ordered distribution inside a 1D optical lattice. The atom-sorting procedure works akin to Maxwell’s demon. In essence, an automated feedback-based experimental setup acquires the initial location of atoms through fluorescence imaging with single site precision, and it uses this information to subsequently shift the atoms, one by one, to form the desired pattern. As illustrated in Fig. 1(a), two spatially overlapped optical lattices,

$$U_{\uparrow}(x, t) = U_{\uparrow}^0 \cos^2\{k_L[x - x_{\uparrow}(t)]\}, \quad (1)$$

$$U_{\downarrow}(x, t) = U_{\downarrow}^0 \cos^2\{k_L[x - x_{\downarrow}(t)]\}, \quad (2)$$

with identical lattice constant (π/k_L) are used to sort atoms. The first lattice is kept fixed, serving as a *storage register* for atoms in the hyperfine state $|\uparrow\rangle = |F = 4, m_F = 4\rangle$, while the other one is mobile, providing a *shift register* for atoms in $|\downarrow\rangle = |F = 3, m_F = 3\rangle$. A digitally programmable polarization synthesizer, as will be detailed later, gives us full independent control of both lattice depths U_s ($s \in \{\uparrow, \downarrow\}$) as well as of the lattice positions $x_s(t)$, which are varied in time to shift the atoms. We choose deep lattices, of the order of a thousand recoil energies, to allow fast transport on the time scale of ten microseconds, while preventing intersite tunneling. For each atom we intend to reposition, we flip its spin, $|\uparrow\rangle \rightarrow |\downarrow\rangle$, using a position-resolved microwave pulse [28,38], which transfers it into the shift register. Once the atom is repositioned by translating the shift register, it is transferred back into the storage register through optical pumping. The fluorescence images in Figs. 1(b)–1(e) show the final distribution of atoms for four different target patterns, including the unity filling of a region of the lattice. Between fluorescence images, several sorting operations are carried out with no need to continuously monitor the positions of atoms. If errors are detected in the final distribution (e.g., imperfect spin flips, wrong position reconstruction, atom losses), a feedback control system attempts to correct them.

Experimental apparatus.—A small ensemble of cesium atoms is captured from the background vapor into a magneto-optical trap, and transferred into a 1D optical lattice produced by linearly polarized light at the wavelength $\lambda_L = 2\pi/k_L = 866$ nm. The lifetime of atoms due to collisions with background gas is about 360 s. The lattice depth is chosen equal for both spin species, $U_{\uparrow}^0 = U_{\downarrow}^0 \approx 75 \mu\text{K}$, and significantly larger than the atoms’ temperature, which is about $8 \mu\text{K}$ after molasses cooling. The loading procedure is adjusted to spread the atoms along the lattice with an average separation of around 20 lattice sites. Optical pumping initializes atoms in $|\uparrow\rangle$ state with $> 99\%$ efficiency using a σ^+ -polarized laser. To detect the atoms’ positions, we acquire fluorescence images with 1 s illumination time using an electron-multiplying CCD camera. We employ a super-resolution-microscopy technique [39] to resolve in real time the individual atoms beyond the diffraction limit of around four sites, as can be seen comparing Figs. 1(c) and 1(d). The local addressing of individual atoms is achieved through spectrally narrow Gaussian-shaped microwave pulses (7 kHz rms width) in combination with a weak magnetic field gradient (11.6 G/cm) along the direction of the optical lattice [28]. For the sorting procedure, we select atoms isolated by more than 20 sites to ensure a probability $< 1\%$ that local addressing pulses spin-flip a neighboring atom. We choose adiabatic, sinusoidal ramps to transport the addressed atoms in the shift register in approximately 1 ms,

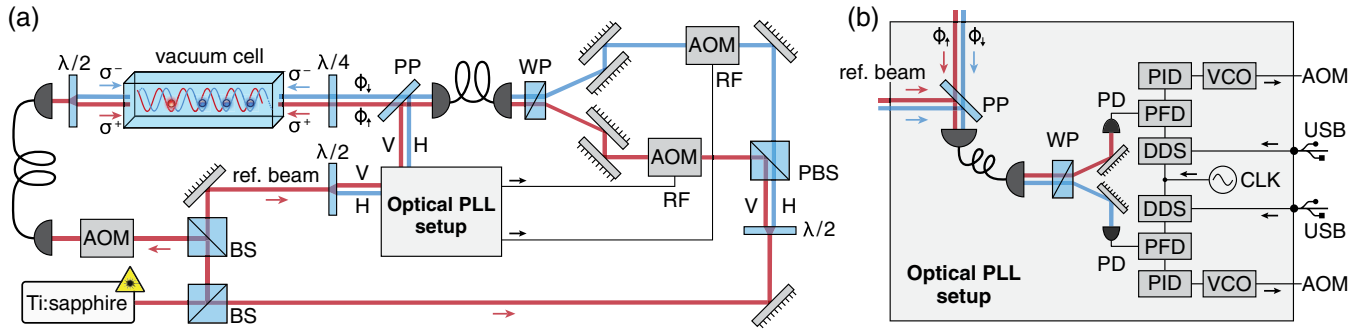


FIG. 2. Schematic illustration of the experimental setup for polarization-synthesized optical lattices. (a) The linearly polarized output of a Ti:sapphire laser is split by beam splitters (BS) into the reference beam, which is used for the optical phase-locked loops (PLLs), and the beams forming the lattice in the vacuum cell. While the polarization of the left lattice beam is static and linear, the polarization of the right lattice beam is synthesized by overlapping two beams of opposite circular polarizations. The latter are combined by a Wollaston prism (WP) in the linear polarization basis (vertical V , horizontal H), spatially mode matched by a polarization maintaining optical fiber (high polarization extinction ratio > 50 dB [45]), and transformed into circular polarizations by a $\lambda/4$ plate. A fraction of light is diverted by a pick-up plate (PP) into the optical PLL setup, which controls the optical phases ϕ_{\uparrow} and ϕ_{\downarrow} by feeding rf signals back to the acousto-optic modulators (AOMs). (b) Optical PLL setup: The diverted light is overlapped with a common reference beam. The resulting beat signals are independently recorded by fast photodiodes (PDs) after the WP. The phase of each beat signal is compared with a rf reference signal (DDS) using a digital phase-frequency discriminator (PFD), and fed to a PID controller (10 MHz bandwidth), which steers the corresponding AOM through a voltage-controlled oscillator (VCO). The DDS rf sources are phase referenced to the same 400 MHz clock signal (CLK) and interfaced via USB with a computer. Three additional control-loop setups (not shown) independently regulate the intensity of each lattice beam by controlling the rf power of the corresponding AOM.

much shorter than the longitudinal spin relaxation time of 100 ms due to inelastic scattering of the lattice photons. We pump atoms back into the storage register by 2-ms-long optical pumping. Atoms in excess are removed from the lattice by first spin-flipping the sorted atoms into the shift register, and by subsequently applying a resonant pulse with the $F = 4 \rightarrow F' = 5$ transition, pushing atoms in the $|\uparrow\rangle$ state out of the optical lattice, while not affecting atoms in the $|\downarrow\rangle$ state. Our deep optical lattice, superimposed with a blue-detuned doughnut-shaped trap, yields longitudinal and transverse trapping frequencies of about $\omega_{\parallel} \approx 2\pi \times 110$ kHz and $\omega_{\perp} \approx 2\pi \times 20$ kHz, well above the recoil frequency $2\pi \times 2$ kHz of cesium. The large trapping frequencies allow us to employ microwave [40] and Raman [41] sideband cooling to cool atoms in the longitudinal and radial directions, respectively, achieving a ground state occupation of 99% along the axial direction and of 80% along each of the two radial directions.

Polarization-synthesized optical lattices.—The key elements in realizing the spin-dependent optical-lattice potentials shown in Eqs. (1) and (2) are two superimposed, yet independently controllable optical standing waves with opposite circular polarizations, σ^{+} and σ^{-} . For both standing waves we choose a so-called magic wavelength λ_L of cesium, allowing atoms in $|\uparrow\rangle$ and $|\downarrow\rangle$ states to be trapped in the maximum-intensity regions of the σ^{+} - and σ^{-} -polarized light field, respectively [42]. Such a wavelength exists because of the different ac vector polarizability of the two internal states [43], and was already employed in earlier implementations of spin-dependent optical lattices (e.g., Refs. [24,25]). However, these implementations permitted only relative

displacements and, most importantly, maximum shift distances of one lattice site, thereby precluding the possibility of sorting randomly distributed atoms into predefined patterns. In contrast, PS optical lattices entirely overcome these limitations by relying on two fully independent optical standing waves. In order to create the standing waves, we let two copropagating laser beams with opposite circular polarization each interfere with a linearly polarized, counter-propagating beam, as illustrated in Fig. 2(a). We employ an optical fiber to ensure that the resulting standing waves are perfectly matched to the same transverse mode, and thereby that atoms in both spin states, $|\uparrow\rangle$ and $|\downarrow\rangle$, experience an identical transverse potential. Transverse-mode filtering is essential to ensure long spin-coherence times for spectrally narrow coherent pulses (e.g., spin flips for single-atom addressing), or else thermal atoms would undergo inhomogeneous spin dephasing in a few microseconds due to a strong differential light shift [44].

While in the transverse directions the two standing waves are perfectly overlapped, they are free to slide with respect to each other in the lattice direction. The position of each standing wave must be controlled with interferometric precision to ensure that atoms are shifted with single-site precision, and that no motional excitation is created when atoms are transferred between the storage and shift registers [42]. We achieve this by employing two independent optical phase-locked loops (PLLs) that actively stabilize the phases of each circularly polarized beam, ϕ_{\uparrow} and ϕ_{\downarrow} , with respect to a common optical reference beam. As shown in Fig. 2(b), each optical phase ϕ_s is referenced to a low-phase-noise rf reference signal (DDS). Varying the

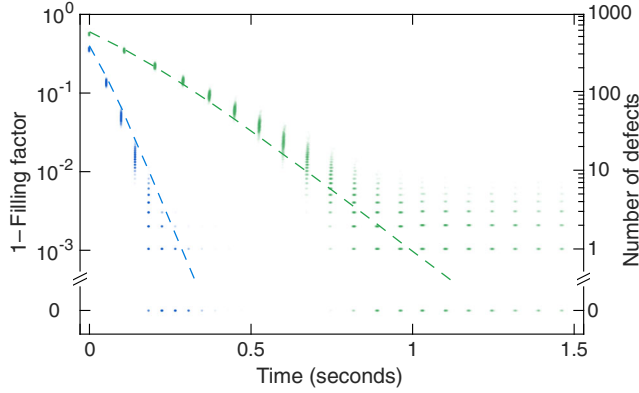


FIG. 3. Monte Carlo simulation of the PSOLAS algorithm filling a square region of a 2D optical lattice with 961 atoms. Upper and lower data sets refer to scenarios (A) and (B) discussed in the text. Dashed lines denote, for each scenario, the exponential law derived in the text. The data show that with 95% probability, defect-free unity filling is reached in less than 0.3 s (A) and 2.2 s (B). In scenario (A), deviations from the exponential law are attributed to the conservative conditions. Nevertheless, the scaling law remains exponential, with a reduced effective filling probability.

phase of the rf signals according to a digitally programmed profile allows us to independently steer ϕ_s , and thereby the position of the respective optical potential U_s :

$$x_s(t) = \frac{\lambda_L}{2} \frac{\phi_s(t)}{2\pi}. \quad (3)$$

A measurement of the relative phase noise $\Delta\phi = \phi_\uparrow - \phi_\downarrow$ yields an uncertainty of 0.1° [46], which translates into a jittering of the relative position of $\Delta x = 1.20 \text{ \AA}$. This is more than 2 orders of magnitude smaller than the extent of the atomic wave function in the vibrational ground state (20 nm) [47]. Moreover, to attest the reliability of the spin-dependent transport operations, we shifted spin-polarized atoms using a single transport operation, chosen to be about 1 ms long, over a distance varying from a few to one hundred sites. We measure a success rate of 97.4(3)%, nearly independent of the distance. We attribute the remaining unsuccessful events to optical pumping errors (0.4%), spin flips during transport (0.6%), and position reconstruction errors (1.6%). This dramatically differs from previously reported transport efficiencies, decreasing exponentially with the transport distance. Even with the best reported efficiency of 99% per shift operation [48], transport efficiency over 20 sites had never exceeded $0.99^{2 \cdot 20} \approx 67\%$.

Thousands of atoms.—While low-entropy states comprising as few as four atoms already suffice to study a wide range of few-body phenomena [16,17,49,50], it is important to discuss how the atom-sorting scheme based on PS optical lattices can be extended to much larger numbers of atoms, thus providing a bottom-up pathway to many-body physics. Compared to recent results [29,30] demonstrating

the sorting of 50 atoms with optical tweezers, fewer atoms are sorted in Fig. 1 because of the limited addressing resolution (20 sites) of the present apparatus (see Supplemental Material [51]). However, we expect that with a higher addressing resolution [52] PS optical lattices allow sorting even thousands of atoms into arbitrary target patterns.

To that purpose, we propose a new atom-sorting algorithm based on PS optical lattices, which rearranges N atoms using a number of operations of the order of $\log N$. The logarithmic complexity is enabled by two properties unique to PS optical lattices, namely, their ability to shift atoms (1) spin dependently and (2) by any arbitrary number of sites; moreover, its logarithmic complexity also holds for two-dimensional (2D) PS optical lattices, which have been recently proposed in Ref. [53]. Hitherto, the best algorithm [54] for sorting atoms in a 2D array requires a larger number of operations of order $N^{1/2}$, because only one-lattice-site shifts are used instead of property (2).

The PS-optical-lattice atom-sorting (PSOLAS) algorithm proposed here iterates four steps: Step 1 identifies, among the atoms not yet sorted, patterns of atoms that best match the distribution of defects, i.e., the empty sites to be filled with one atom; this step requires acquiring the positions of the atoms through a fluorescence image [55]. Step 2 transfers the identified atoms from the storage register into the shift register; this step can be performed in parallel by optically addressing atoms using a spatial light modulator [56,57] or serially using a beam deflector [29,58]. Step 3 shifts the whole pattern of selected atoms, in parallel, to fill the defects; this step is the crucial one, which is enabled by the properties (1) and (2) of PS optical lattices. Step 4 transfers the shifted atoms into the storage register by optical pumping. An illustrative demonstration of the PSOLAS algorithm to fill a square region of a 2D optical lattice is provided in the Supplemental Material [51].

Since the duration of each step is independent from the number of sorted atoms for a broad parameter range, the overall time required by PSOLAS is determined by the number of iterations. The latter is estimated by considering that each iteration fills, on average, a fraction α of the defects in the target pattern, where α denotes the initial filling probability of a lattice site. In reality, because the algorithm searches for the best matching pattern of atoms to shift, the fraction of filled defects per iteration is generally higher than α . Hence, the number of defects after n iterations amounts to less than $N(1 - \alpha)^{1+n}$, meaning that to attain a number of defect of the order of $\mathcal{O}(1)$, about $\mathcal{O}(\log N)$ iterations are required. To validate this scaling law under realistic conditions, we carried out Monte Carlo simulations in two scenarios representing (A) conservative and (B) state-of-the-art conditions; the conditions of both scenarios are derived from individual results demonstrated either in our or other laboratories. In both scenarios, PSOLAS aims to fill a square target pattern of 31×31 sites by “tapping” into the atoms

stored in a larger region of 100×100 sites. Scenarios (A) and (B) rely on 80% and 95% [58] single-site addressing efficiency, and the filling probability α is chosen equal to 40% and 60% [20], respectively (all parameters are summarized in the Supplemental Material [51]). As shown in Fig. 3, we find that even in scenario (A), about 1000 atoms can be sorted in a time of about 1 s.

Conclusions.—In this Letter, we demonstrated a bottom-up approach to the generation of low-entropy states of ultracold atoms in optical lattices. Our work demonstrates that arbitrary filling patterns with virtually zero entropy can be realized experimentally. The key to our sorting procedure is the development of PS optical lattices, which provide us with a new set of operations for the control of atoms depending on their spin orientation. Presently, the entropy of our prepared states is limited by the vibrational entropy [59] due to the limited efficiency (60%) of the sideband cooling into the three-dimensional vibrational ground state. A tighter optical confinement of atoms shall enable significantly higher efficiencies. The construction of a 2D PS optical lattice is underway [53] in a new experimental apparatus, which additionally features a high optical resolution objective lens for optical single-site addressing [52]; this should allow us to demonstrate PSOLAS with thousands of atoms.

We thank A. Hambitzer for contributing to the experimental apparatus and S. Hild, A. Steffen, G. Ramola, M. Tarallo, J. M. Raimond, and C. Kollath for insightful discussions. We acknowledge financial support from the NRW-Nachwuchsforschergruppe “Quantenkontrolle auf der Nanoskala,” the ERC grant DQSIM, the EU SIQS project, and the Deutsche Forschungsgemeinschaft SFB project OSCAR. C. R. acknowledges support from the Studienstiftung des deutschen Volkes, and C. R., S. B., and J. Z. from the Bonn-Cologne Graduate School.

C. R. and J. Z. contributed equally to this work.

*alberti@iap.uni-bonn.de

- [1] I. Bloch and P. Zoller, Ultracold Atoms and Molecules in Optical Lattices, in *Ultracold Bosonic and Fermionic Gases*, edited by K. Levin, A. L. Fetter, and D. M. Stamper-Kurn (Elsevier, New York, 2012), p. 121.
- [2] H. Katori, Optical lattice clocks and quantum metrology, *Nat. Photonics* **5**, 203 (2011).
- [3] D. Jaksch, H.-J. Briegel, J. I. Cirac, C. W. Gardiner, and P. Zoller, Entanglement of Atoms via Cold Controlled Collisions, *Phys. Rev. Lett.* **82**, 1975 (1999).
- [4] G. K. Brennen, C. M. Caves, P. S. Jessen, and I. H. Deutsch, Quantum Logic Gates in Optical Lattices, *Phys. Rev. Lett.* **82**, 1060 (1999).
- [5] R. Raussendorf and H. J. Briegel, A One-Way Quantum Computer, *Phys. Rev. Lett.* **86**, 5188 (2001).
- [6] J. H. Lee, E. Montano, I. H. Deutsch, and P. S. Jessen, Robust site-resolvable quantum gates in an optical lattice via inhomogeneous control, *Nat. Commun.* **4**, 2027 (2013).
- [7] T. Xia, M. Lichtman, K. Maller, A. W. Carr, M. J. Piotrowicz, L. Isenhower, and M. Saffman, Randomized Benchmarking of Single-Qubit Gates in a 2D Array of Neutral-Atom Qubits, *Phys. Rev. Lett.* **114**, 100503 (2015).
- [8] Y. Wang, A. Kumar, T. Y. Wu, and D. S. Weiss, Single-qubit gates based on targeted phase shifts in a 3D neutral atom array, *Science* **352**, 1562 (2016).
- [9] M. Karski, L. Förster, J. Choi, A. Steffen, W. Alt, D. Meschede, and A. Widera, Quantum Walk in Position Space with Single Optically Trapped Atoms, *Science* **325**, 174 (2009).
- [10] D. Jaksch, C. Bruder, J. I. Cirac, C. W. Gardiner, and P. Zoller, Cold Bosonic Atoms in Optical Lattices, *Phys. Rev. Lett.* **81**, 3108 (1998).
- [11] M. Greiner, O. Mandel, T. Esslinger, T. W. Hänsch, and I. Bloch, Quantum phase transition from a superfluid to a Mott insulator in a gas of ultracold atoms, *Nature (London)* **415**, 39 (2002).
- [12] M. Lewenstein, A. Sanpera, and V. Ahufinger, *Ultracold Atoms in Optical Lattices* (Oxford University Press, New York, 2012).
- [13] W. S. Bakr, A. Peng, M. E. Tai, R. Ma, J. Simon, J. I. Gillen, S. Fölling, L. Pollet, and M. Greiner, Probing the Superfluid-to-Mott Insulator Transition at the Single-Atom Level, *Science* **329**, 547 (2010).
- [14] J. F. Sherson, C. Weitenberg, M. E. M. Cheneau, I. Bloch, and S. Kuhr, Single-atom-resolved fluorescence imaging of an atomic Mott insulator, *Nature (London)* **467**, 68 (2010).
- [15] O. Mandel, M. Greiner, A. Widera, T. Rom, T. Hänsch, and I. Bloch, Controlled collisions for multi-particle entanglement of optically trapped atoms, *Nature (London)* **425**, 937 (2003).
- [16] A. M. Kaufman, B. J. Lester, C. Reynolds, M. L. Wall, M. Foss-Feig, K. R. A. Hazzard, A. M. Rey, and C. A. Regal, Two-particle quantum interference in tunnel-coupled optical tweezers, *Science* **345**, 306 (2014).
- [17] R. Islam, R. Ma, P. M. Preiss, M. E. Tai, A. Lukin, M. Rispoli, and M. Greiner, Measuring entanglement entropy in a quantum many-body system, *Nature (London)* **528**, 77 (2015).
- [18] A. Leggett, *Quantum Liquids: Bose Condensation and Cooper Pairing in Condensed-Matter Systems* (Oxford University Press, New York, 2006).
- [19] T. Esslinger, Fermi-Hubbard Physics with Atoms in an Optical Lattice, *Annu. Rev. Condens. Matter Phys.* **1**, 129 (2010).
- [20] Y. Fung, P. Sompert, and M. Andersen, Single Atoms Preparation Using Light-Assisted Collisions, *Technologies de l'Information et Societe* **4**, 4 (2016).
- [21] M. T. DePue, C. McCormick, S. L. Winoto, S. Oliver, and D. S. Weiss, Unity Occupation of Sites in a 3D Optical Lattice, *Phys. Rev. Lett.* **82**, 2262 (1999).
- [22] A. Fuhrmanek, R. Bourgain, Y. R. P. Sortais, and A. Browaeys, Light-assisted collisions between a few cold atoms in a microscopic dipole trap, *Phys. Rev. A* **85**, 062708 (2012).
- [23] D. S. Weiss, J. Vala, A. V. Thapliyal, S. Myrgren, U. Vazirani, and K. B. Whaley, Another way to approach zero entropy for a finite system of atoms, *Phys. Rev. A* **70**, 040302 (2004).

- [24] O. Mandel, M. Greiner, A. Widera, T. Rom, T. W. Hänsch, and I. Bloch, Coherent Transport of Neutral Atoms in spin-dependent optical lattice potentials, *Phys. Rev. Lett.* **91**, 010407 (2003).
- [25] A. Steffen, A. Alberti, W. Alt, N. Belmechri, S. Hild, M. Karski, A. Widera, and D. Meschede, A digital atom interferometer with single particle control on a discretized spacetime geometry, *Proc. Natl. Acad. Sci. U.S.A.* **109**, 9770 (2012).
- [26] Y. Miroshnychenko, W. Alt, I. Dotsenko, L. Förster, M. Khudaverdyan, D. Meschede, D. Schrader, and A. Rauschenbeutel, Quantum engineering: An atom-sorting machine, *Nature (London)* **442**, 151 (2006).
- [27] D. Schrader, I. Dotsenko, M. Khudaverdyan, Y. Miroshnychenko, A. Rauschenbeutel, and D. Meschede, Neutral Atom Quantum Register, *Phys. Rev. Lett.* **93**, 150501 (2004).
- [28] M. Karski, L. Förster, J. Choi, A. Steffen, N. Belmechri, W. Alt, D. Meschede, and A. Widera, Imprinting patterns of neutral atoms in an optical lattice using magnetic resonance techniques, *New J. Phys.* **12**, 065027 (2010).
- [29] D. Barredo, S. de Léséleuc, V. Lienhard, T. Lahaye, and A. Browaeys, An atom-by-atom assembler of defect-free arbitrary 2D atomic arrays., *Science* **354**, 1021 (2016).
- [30] M. Endres, H. Bernien, A. Keesling, H. Levine, E. R. Anschuetz, A. Krajenbrink, C. Senko, V. Vuletić, M. Greiner, and M. D. Lukin, Atom-by-atom assembly of defect-free one-dimensional cold atom arrays, *Science* **354**, 1024 (2016).
- [31] M. Saffman, Quantum computing with atomic qubits and Rydberg interactions: Progress and challenges, *J. Phys. B* **49**, 202001 (2016).
- [32] A. Gaëtan, Y. Miroshnychenko, T. Wilk, A. Chotia, M. Viteau, D. Comparat, P. Pillet, A. Browaeys, and P. Grangier, Observation of collective excitation of two individual atoms in the Rydberg blockade regime, *Nat. Phys.* **5**, 115 (2009).
- [33] E. Urban, T. A. Johnson, T. Henage, L. Isenhower, D. D. Yavuz, T. G. Walker, and M. Saffman, Observation of Rydberg blockade between two atoms, *Nat. Phys.* **5**, 110 (2009).
- [34] A. Alberti, V. V. Ivanov, G. M. Tino, and G. Ferrari, Engineering the quantum transport of atomic wavefunctions over macroscopic distances, *Nat. Phys.* **5**, 547 (2009).
- [35] B. Horstmann, S. Dürr, and T. Roscilde, Localization of Cold Atoms in State-Dependent Optical Lattices via a Rabi Pulse, *Phys. Rev. Lett.* **105**, 160402 (2010).
- [36] I. de Vega, D. Porras, and J. I. Cirac, Matter-Wave Emission in Optical Lattices: Single Particle and Collective Effects, *Phys. Rev. Lett.* **101**, 260404 (2008).
- [37] T. Shi, Y.-H. Wu, A. González-Tudela, and J. I. Cirac, Bound States in Boson Impurity Models, *Phys. Rev. X* **6**, 021027 (2016).
- [38] M. Johanning, A. Braun, N. Timoney, V. Elman, W. Neuhauser, and C. Wunderlich, Individual Addressing of Trapped Ions and Coupling of Motional and Spin States Using rf Radiation, *Phys. Rev. Lett.* **102**, 073004 (2009).
- [39] A. Alberti, C. Robens, W. Alt, S. Brakhane, M. Karski, R. Reimann, A. Widera, and D. Meschede, Super-resolution microscopy of single atoms in optical lattices, *New J. Phys.* **18**, 053010 (2016).
- [40] L. Förster, M. Karski, J.-M. Choi, A. Steffen, W. Alt, D. Meschede, A. Widera, E. Montano, J. H. Lee, W. Rakreungdet, and P. S. Jessen, Microwave Control of Atomic Motion in Optical Lattices, *Phys. Rev. Lett.* **103**, 233001 (2009).
- [41] A. M. Kaufman, B. J. Lester, and C. A. Regal, Cooling a Single Atom in an Optical Tweezer to its Quantum Ground State, *Phys. Rev. X* **2**, 041014 (2012).
- [42] N. Belmechri, L. Förster, W. Alt, A. Widera, D. Meschede, and A. Alberti, Microwave control of atomic motional states in a spin-dependent optical lattice, *J. Phys. B* **46**, 104006 (2013).
- [43] I. H. Deutsch and P. S. Jessen, Quantum-state control in optical lattices, *Phys. Rev. A* **57**, 1972 (1998).
- [44] A. Alberti, W. Alt, R. Werner, and D. Meschede, Decoherence Models for Discrete-Time Quantum Walks and their Application to Neutral Atom Experiments, *New J. Phys.* **16**, 123052 (2014).
- [45] F. M. Sears, Polarization-maintenance limits in polarization-maintaining fibers and measurements, *J. Lightwave Technol.* **8**, 684 (1990).
- [46] C. Robens, S. Brakhane, W. Alt, D. Meschede, J. Zopes, and A. Alberti, Fast, high-precision optical polarization synthesizer for ultracold-atom experiments, [arXiv:1611.07952](https://arxiv.org/abs/1611.07952).
- [47] The relative position jitter must be much smaller than the harmonic oscillator length $\sqrt{\hbar/(2m\omega_{\parallel})}$, with m being the mass of the atom.
- [48] M. Karski, L. Förster, J. Choi, W. Alt, A. Alberti, A. Widera, and D. Meschede, Direct observation and analysis of spin-dependent transport of single atoms in a 1D optical lattice, *J. Korean Phys. Soc.* **59**, 2947 (2011).
- [49] S. Murmann, A. Bergschneider, V. M. Klinkhamer, G. Zürn, T. Lompe, and S. Jochim, Two Fermions in a Double Well: Exploring a Fundamental Building Block of the Hubbard Model, *Phys. Rev. Lett.* **114**, 080402 (2015).
- [50] S. Murmann, F. Deuretzbacher, G. Zürn, J. Bjerlin, S. M. Reimann, L. Santos, T. Lompe, and S. Jochim, Antiferromagnetic Heisenberg Spin Chain of a Few Cold Atoms in a One-Dimensional Trap, *Phys. Rev. Lett.* **115**, 215301 (2015).
- [51] See Supplemental Material at <http://link.aps.org/supplemental/10.1103/PhysRevLett.118.065302> for further information about the atom-sorting algorithm PSOLAS.
- [52] C. Robens, S. Brakhane, W. Alt, F. Kleibler, D. Meschede, G. Moon, G. Ramola, and A. Alberti, A high numerical aperture (NA = 0.92) objective lens for imaging and addressing of cold atoms, [arXiv:1611.02159](https://arxiv.org/abs/1611.02159).
- [53] T. Groh, S. Brakhane, W. Alt, D. Meschede, J. K. Asbóth, and A. Alberti, Robustness of topologically protected edge states in quantum walk experiments with neutral atoms, *Phys. Rev. A* **94**, 013620 (2016).
- [54] J. Vala, A. V. Thapliyal, S. Myrgren, U. Vazirani, D. S. Weiss, and K. B. Whaley, Perfect pattern formation of neutral atoms in an addressable optical lattice, *Phys. Rev. A* **71**, 032324 (2005).
- [55] Note that a fluorescence image is not strictly required at each iteration since atoms can also be sorted blindly for several iterations, as we demonstrated in Fig. 1.
- [56] G. Gauthier, I. Lenton, N. M. Parry, M. Baker, M. J. Davis, H. Rubinsztein-Dunlop, and T. W. Neely, Direct imaging of

- a digital-micromirror device for configurable microscopic optical potentials, *Optica* **3**, 1136 (2016).
- [57] F. Nogrette, H. Labuhn, S. Ravets, D. Barredo, L. Béguin, A. Vernier, T. Lahaye, and A. Browaeys, Single-Atom Trapping in Holographic 2D Arrays of Microtraps with Arbitrary Geometries, *Phys. Rev. X* **4**, 021034 (2014).
- [58] C. Weitenberg, M. Endres, J.F. Sherson, M. Cheneau, P. Schauß, T. Fukuhara, I. Bloch, and S. Kuhr, Single-spin addressing in an atomic Mott insulator, *Nature (London)* **471**, 319 (2011).
- [59] M. Olshanii and D. Weiss, Producing Bose-Einstein Condensates Using Optical Lattices, *Phys. Rev. Lett.* **89**, 090404 (2002).

Supplemental Material for: Low-entropy states of neutral atoms in polarization-synthesized optical lattices

Carsten Robens^{1,†}, Jonathan Zopes^{1,†}, Wolfgang Alt¹, Stefan Brakhane¹, Dieter Meschede¹, and Andrea Alberti^{1,*}

¹*Institut für Angewandte Physik, Universität Bonn, Wegelerstr. 8, D-53115 Bonn, Germany*

SI. LOCAL ADDRESSING OF INDIVIDUAL ATOMS

The microwave addressing resolution of 20 lattice sites given in the main text limits the maximum number of atoms that we can sort in a low-entropy state. Our imaging system’s field of view spans over 160 lattice sites, which corresponds to 8 atoms separated by 20 sites. However, the situation of 8 atoms equally separated is extremely improbable since atoms are initially distributed in random positions. Thus, with the experimental apparatus presently at hand we are limited to between 4 and 6 atoms.

With the same experimental apparatus, we have demonstrated in the past much higher addressing resolutions, by working with magnetic field gradients about a factor 20 higher [28]. The technical challenge using high magnetic field gradients resides in the long time (more than 100 ms) required to ramp up or down the magnetic field, during which off-resonant scattering of lattice photons can occur ($T_1 \approx 100$ ms). This is not a problem for atoms sorted in distinct lattice sites, since they can be reinitialized into the motional ground state by sideband cooling. However, it poses a limitation for sorting two or more ground-state-cooled atoms into the same lattice site, since the subsequent application of sideband cooling would lead to highly detrimental losses by light-assisted collisions instead of reinitializing atoms into the ground state. Hence, for our atom-sorting demonstration, we opted for a rather weak magnetic field gradient, which enables in the future the study of intriguing many-body effects.

Moreover, switching from magnetic field gradients to tightly focused laser beams employing a high-NA objective lens [52] should allow us to achieve local addressing with single-lattice-site resolution.

	Conservative	State of the art
Image acquisition time	60 ms	30 ms
Addressing efficiency	80 %	95 %
Addressing crosstalk	10 %	5 %
Initial filling probability	40 %	60 %
Storage time	60 s	360 s
Duration of optical pumping	10 ms	10 ms
Duration of lattice shift	1 ms	1 ms
Addressing duration	150 μ s	30 μ s

TABLE. S1. Monte Carlo simulation parameters of PSOLAS for a conservative and a state-of-the-art scenario, as described in Sec. SII.

SII. MONTE CARLO SIMULATIONS OF PSOLAS

We carried out Monte Carlo simulations of the PS-optical-lattice atom-sorting (PSOLAS) algorithm using the parameters reported in Tab. S1 for two different scenarios based on either conservative or state-of-the-art conditions. As mentioned in the main text, we have chosen the conditions of both scenarios based on individual results obtained either in our or other laboratories.

We are currently setting up a two-dimensional (2D) polarization-synthesized (PS) optical lattice experimental apparatus, which is designed to reach the experimental conditions described in the state-of-the-art scenario [53]. A key component of our new experimental apparatus is a custom-built objective lens with high numerical aperture NA=0.92 [52]. The objective lens achieves a diffraction limited resolution of 460 nm, compared to the lattice constant of 612 nm, and increases the photon collection efficiency by a factor 30 compared to that obtained with the apparatus described in the main text. Consequently, we expect a significant improvement in the localization precision, allowing us to determine the lattice position of individual atoms in few tens of milliseconds. Furthermore, the high-NA objective lens should enable us to address individual atoms with high efficiency using tightly focused laser beams, which induces a differential light shift for the addressed atoms [58]. It was recently demonstrated that the efficiency of this technique can exceed 99 % [8]. Thus, we assumed in our Monte Carlo simulations an addressing efficiency of 80 % and 95 % for the two scenarios. We additionally accounted for an addressing crosstalk of 5 % or 10 %, which leads to unwanted spin flips of neighboring atoms. Moreover, the region of 100×100 sites considered in the Monte Carlo simulations corresponds to the field of view of our high-NA objective lens.

The initial filling probability of the lattice is determined by the density of atoms that are initially captured in the magneto-optical trap and by the efficiency of the so-called parity projection caused by light-assisted collisions. In our current implementation we found initial filling probabilities to vary between 40 % and 65 %. Notably, Fung *et al.* [20] show that initial filling probabilities exceeding 80 % can be realized using an additional blue-detuned laser beam while loading atoms from the magneto-optical trap into the optical lattice.

With the experimental apparatus described in the main text, we achieve storage times in the range of 360 s due to the ultra-high vacuum conditions realized in the “science” cell, where the partial vacuum pressure of Cs atoms is very low. With the new 2D experimental apparatus, we expect to achieve storage times of the order of one minute.

The chosen duration of optical pumping (10 ms) and that of a lattice shift operation (1 ms) match the settings of the experiments reported in the main text. For serial

* alberti@iap.uni-bonn.de; †Both authors contributed equally to this work.

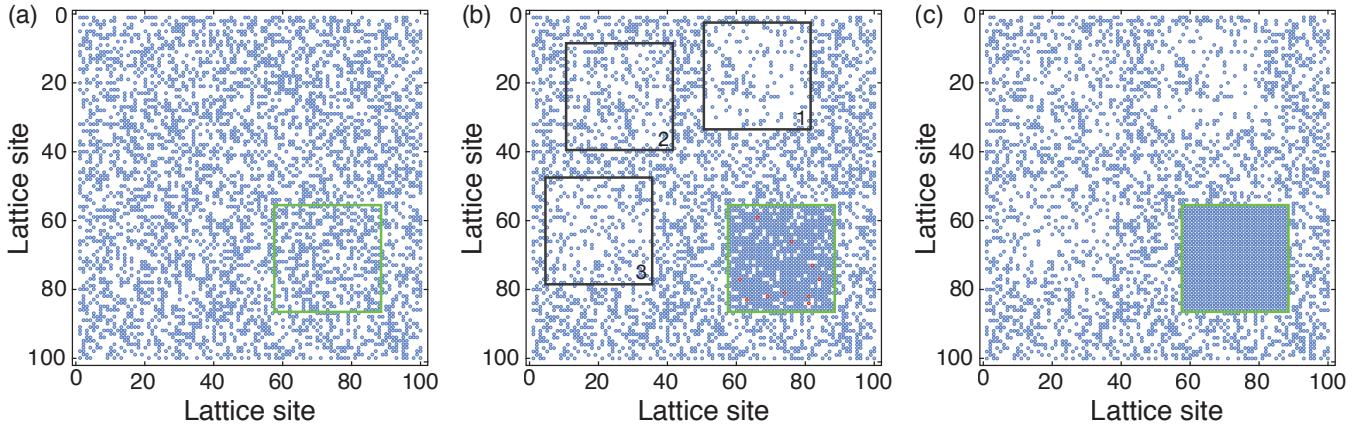


FIG. S1. Conceptual illustration of PSOLAS using the conservative parameters given in Tab. S1. The goal is to create unity filling in a square target pattern of 31×31 lattice sites (green square region). (a) Initial distribution of atoms in a 2D optical lattice with 40% initial filling probability. (b) Atom distribution after 3 PSOLAS iterations. The black squares represent the regions where the atom patterns best matched the remaining holes in the target region. The red pixels indicate lattice sites with double occupancy, which are caused from addressing crosstalk at the third iteration of PSOLAS. In our Monte Carlo simulations, we assumed perfect parity projection; hence these lattice sites will result in holes at the next iteration of PSOLAS. (c) Final atom distribution with unity filling of 961 lattices sites (31×31) obtained after 12 PSOLAS iterations.

addressing, the addressing duration depends on how fast one can steer the laser beam generating the local differential light shift and the duration of the subsequently applied microwave pulse itself. Previous demonstrations of the addressing scheme achieved local differential light shifts of ≈ 60 kHz [58]. In this case, microwave pulses with a duration of $30 \mu\text{s}$ have the required frequency resolution to ensure low addressing crosstalk. As a conservative assumption, we take the current microwave pulse duration of $150 \mu\text{s}$, which correspond to smaller AC Stark-shifts. In both scenarios, the beam steering duration can be neglected due to the high bandwidth of acousto-optic modulators (steering time $< 1 \mu\text{s}$). Furthermore, we note that spatial light modulators [56, 57] (e.g., liquid crystal on silicon operated in amplitude modulation mode, with refresh rates of $\gtrsim 10$ Hz) could also enable parallel addressing of hundreds of atoms by imaging the square grid of pixels onto the square two-dimensional optical lattice.

For the complexity estimate of PSOLAS, we neglected the computational time required to process, e.g., atom positions, which can be efficiently performed by a CPU or in parallel by a dedicated FPGA chip. This computational time is much shorter than the other time scales.

III. ILLUSTRATION OF PSOLAS

In Fig. S1, we provide a graphical illustration of the working principle of PSOLAS algorithm under the conservative conditions (see Tab. S1) to accompany the description given in the main text. For the chosen example, we use PSOLAS to create unity filling in a square target pattern of 31×31 lattice sites, repositioning atoms taken from within a region of 100×100 lattice sites. The three images in the figure are Monte Carlo-simulated atom distributions at the initial time, after three iterations of the algorithm, and at the completion of the algorithm. The initial distribution, see Fig. S1(a), is a random distribution of atoms with an initial filling probability of 40%. PSOLAS chooses the initially densest region of 31×31 lattice sites as the target region, which is indicated by a green rectangle in the figure. The atom distribution

after three iterations, see Fig. S1(b), shows a highly increased density in the target region, whereas a visible depletion in the other square regions indicated by numbers 1, 2, 3, identified by PSOLAS as those regions with atom patterns best matching the distribution of the remaining holes of the target region. In Fig. S1(c), we show the final distribution with perfect unity filling in the target region after 12 iterations of PSOLAS algorithm.

BIBLIOGRAPHY

- [8] Y. Wang, A. Kumar, T. Y. Wu, and D. S. Weiss, Single-qubit gates based on targeted phase shifts in a 3D neutral atom array, *Science* **352**, 1562 (2016).
- [20] Y. H. Fung, P. Sompet, and M. Andersen, Single Atoms Preparation Using Light-Assisted Collisions, *Technologies* **4**, 4 (2016).
- [28] M. Karski, L. Förster, J. Choi, A. Steffen, N. Belmechri, W. Alt, D. Meschede, and A. Widera, Imprinting Patterns of Neutral Atoms in an Optical Lattice using Magnetic Resonance Techniques, *New J. Phys.* **12**, 065027 (2010).
- [52] C. Robens, S. Brakhane, W. Alt, F. Kleißler, D. Meschede, G. Moon, G. Ramola, and A. Alberti, A high numerical aperture ($\text{NA} = 0.92$) objective lens for imaging and addressing of cold atoms, [arXiv:1611.02159](https://arxiv.org/abs/1611.02159).
- [53] T. Groh, S. Brakhane, W. Alt, D. Meschede, J. K. Asbóth, and A. Alberti, Robustness of topologically protected edge states in quantum walk experiments with neutral atoms, *Phys. Rev. A* **94**, 013620 (2016).
- [56] G. Gauthier, I. Lenton, N. M. Parry, M. Baker, M. J. Davis, H. Rubinsztein-Dunlop, and T. W. Neely, Direct imaging of a digital-micromirror device for configurable microscopic optical potentials, *Optica* **3**, 1136 (2016).
- [57] F. Nogrette, H. Labuhn, S. Ravets, D. Barredo, L. Béguin, A. Vernier, T. Lahaye, and A. Browaeys, Single-Atom Trapping in Holographic 2D Arrays of Microtraps with Arbitrary Geometries, *Phys. Rev. X* **4**, 021034 (2014).
- [58] C. Weitenberg, M. Endres, J. F. Sherson, M. Cheneau, P. Schauß, T. Fukuhara, I. Bloch, and S. Kuhr, “Single-spin addressing in an atomic Mott insulator,” *Nature (London)* **471**, 319 (2011).